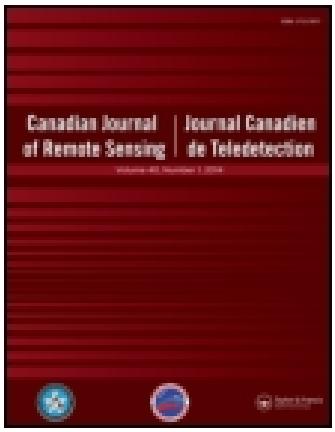

Canadian Journal of Remote Sensing: Journal canadien de télédétection
Publication details, including instructions for authors and subscription information:
http://www.tandfonline.com/loi/ujrs20

Modeling the dielectric behavior of saline soil at microwave frequencies

Huaze Gong[a], Yun Shao[a], Brian Brisco[b], Qingrong Hu[c] & Wei Tian[a]

[a] State Key Laboratory of Remote Sensing Science, Institute of Remote Sensing Applications, Chinese Academy of Sciences, Beijing 100101, China.

[b] Canada Centre for Remote Sensing, Earth Sciences Sector, Natural Resources Canada, 588 Booth Street, Ottawa, ON K1A 0Y7, Canada.

[c] China Aerospace Science and Industry Corporation, Beijing, China.

Published online: 04 Jun 2014.

To cite this article: Huaze Gong, Yun Shao, Brian Brisco, Qingrong Hu & Wei Tian (2013) Modeling the dielectric behavior of saline soil at microwave frequencies, Canadian Journal of Remote Sensing: Journal canadien de télédétection, 39:1, 17-26, DOI: 10.5589/m13-004

To link to this article: http://dx.doi.org/10.5589/m13-004

Can. J. Remote Sensing, Vol. 39, No. 1, pp. 17–26, 2013

Modeling the dielectric behavior of saline soil at microwave frequencies

Huaze Gong, Yun Shao, Brian Brisco, Qingrong Hu, and Wei Tian

Abstract. Soil salinization is a problem of global concern because of the economic impact and, consequently, its measurement and possible control are very important. Electromagnetic sensors such as ground penetrating radar and electromagnetic induction sensors are among the most widely used methods for the detection of soil components. This paper focuses on the dielectric behavior of saline soil at microwave frequencies. Five different soil types with varying levels of moisture and salinity were prepared in the laboratory and their dielectric properties were measured to evaluate the influence of moisture and salinity on the real and imaginary parts of the dielectric constant. An improved dielectric model for saline soil in the microwave frequency range was then developed (with two groups of equations for low- and high-frequency regions) with the regression parameters derived using the Levenberg–Marquardt and Universal Global Optimization methods. This modified model proved to be suitable for saline soil with a good degree of accuracy based on the statistics (R^2 and root mean square error) for both frequency ranges. For example, for the C band (5.25 GHz), discussion on how to use the improved dielectric model at moderate frequency is conducted. Future rigorous experiments under varying field conditions will be conducted to develop a more robust model for implementation using SAR remote sensing technology.

Résumé. La salinisation des sols est un problème d'intérêt mondial en raison des impacts économiques qu'elle engendre et, par conséquent, sa mesure et potentiellement son contrôle sont d'une grande importance. Les capteurs électromagnétiques, tels que le radar pénétrant GPR et les capteurs d'induction électromagnétique, sont parmi les méthodes les plus largement utilisées pour la détection des composantes du sol. Dans cet article, on met l'accent sur le comportement diélectrique des sols salins dans les fréquences microondes. Cinq types de sol différents avec des niveaux variables d'humidité et de salinité ont été préparés en laboratoire et leurs propriétés diélectriques ont été mesurées afin d'évaluer l'influence de l'humidité et de la salinité sur les parties réelles et imaginaires de la constante diélectrique. Un modèle diélectrique amélioré pour les sols salins opérant dans le domaine des fréquences microondes a ensuite été développé (avec deux groupes d'équations pour les régions des basses et des hautes fréquences) utilisant les paramètres de régression dérivés à l'aide des méthodes de Levenberg–Marquardt et d'optimisation globale UGO (« Universal Global Optimization »). Ce modèle modifié s'est avéré utile pour les sols salins affichant un bon degré de précision basé sur les statistiques (R^2 et erreur quadratique moyenne) pour les deux intervalles de fréquences. À titre d'exemple, à l'aide de la bande C (5,25 GHz), on montre comment utiliser le modèle diélectrique amélioré à des fréquences moyennes. D'autres expériences rigoureuses seront menées dans des conditions variables de terrain afin de développer un modèle plus robuste en utilisant les technologies de la télédétection radar à synthèse d'ouverture.
[Traduit par la Rédaction]

Introduction

Salinization and alkalization of soil is a problem of global concern because it is widespread and has significant economic impact. Consequently the accurate measurement of soil salinity for management and, subsequently, the possibility for control are very important (Fariften et al., 2006; Metternicht and Zinck, 2003). Electromagnetic sensors, such as ground penetrating radar sensors and electromagnetic induction sensors, are among the most widely used methods for the detection of soil components (Lesch et al., 1992; Triantafilis et al., 2001; Triantafilis and Lesch, 2005). To predict the performance of electromagnetic sensors, it is common to estimate the soil dielectric properties using models. However, although there are many available models, each with its own particular characteristics, the lack of dielectric models of moist saline soil makes it difficult to delineate the components of such soil using satellite images (Van Dam et al., 2005).

Received 9 September 2012. Accepted 3 February 2013. Published on the Web at http://pubs.casi.ca/journal/cjrs on 25 April 2013.

Huaze Gong[1], Yun Shao, and Wei Tian. State Key Laboratory of Remote Sensing Science, Institute of Remote Sensing Applications, Chinese Academy of Sciences, Beijing 100101, China.

Brian Brisco. Canada Centre for Remote Sensing, Earth Sciences Sector, Natural Resources Canada, 588 Booth Street, Ottawa, ON K1A 0Y7, Canada.

Qingrong Hu. China Aerospace Science and Industry Corporation, Beijing, China.

[1]Corresponding author (e-mail: gonghz@irsa.ac.cn).

Synthetic aperture radar (SAR) remote sensing technology is viewed as a useful tool for implementing Earth observation programs. SAR is sensitive to the geometric and dielectric properties of the targets within the image with the dielectric properties related to the specific moisture and salinity characteristics of the targets. Over the last two decades researchers have worked to apply this technology to a variety of applications and have therefore generated both theoretical and practical models (Dobson et al., 1985; Dubois et al., 1995; Fung et al., 1992; Hallikainen et al., 1985; Oh et al., 1992; Peplinski et al., 1995; Ulaby et al., 1981; Shi et al., 1997; Tsang et al., 1985). Soil salinity is an important factor affecting the dielectric constant, particularly the imaginary part (ε''). However, compared with the large amount of research on moisture retrieval, few attempts have been made to describe the effects of salinity on SAR backscattering. In general, microwave C, P, and especially L bands, are considered adequate for detecting salinity in different settings (Metternicht, 1998; Schmullius and Evans, 1997; Taylor et al., 1996). Metternicht and Zinck, (2003) concluded that previous studies mainly focused on three features, which were saline water detection, soil salinity identification, and soil salinity mapping. Based on laboratory measurements, Shao et al. (2003) concluded that soil moisture strongly affected the real part of dielectric constant (ε'), while the imaginary part (ε'') was controlled by both moisture and salinity, especially at low frequencies. Aly et al. (2007) argued that the existing scattering models did not consider the weight of ε'' adequately, and a new model needed to be developed to determine the salt content of soil. More recently, Lasne et al. (2008) conducted a series of laboratory experiments to analyze characteristics of ε' and ε''. The authors simulated the radar backscattering coefficients by means of the integral equation model. These studies highlighted the feasibility of salinity retrieval using SAR remote sensing technology.

Soil dielectric models are essential components of many algorithms for retrieving soil components from remote sensing data (Mironov et al., 2004). The four-component mixing model is a physical model. Although it could describe principles of dielectric behavior in detail, not all of the input quantities were readily available for specific soil, and some of these parameters were not constant over time for a given soil (Dobson et al., 1985). A generalized refractive mixing dielectric model (GRMDM) based on the Debye formula was applied for estimating the relaxation spectra related to the bound water and free water in soil. A key factor in developing the GRMDM was the technique proposed for calculating the conductivities, relaxation times, and static dielectric constant with the use of a regular soil dielectric constant as a function of soil moisture (Mironov et al., 2004). Dobson developed a relatively simple semi-empirical model based on a physical model that simplified soil systems and simulated dielectric behavior to some extent (Dobson et al., 1985). All the models noted above were from the point of view of nonsaline soil. Researchers have shown that the salinity of soil is the primary factor affecting ε'', and for moist saline soil, salinity factors should not be neglected. Stogryn (1970) developed equations for calculating the dielectric constant of saline water and proposed that the dielectric constant of saline water may be represented by a formula of the Debye form. This proposal generated opportunities to introduce a salinity factor into the dielectric model.

In this study the dielectric properties of moist saline soil samples combined with soil physics and some appropriate simplifications were used to develop an improved model for the dielectric behavior of saline soil at microwave frequencies (with two groups of equations at low and high frequency). The partial data measured from the soil samples in the laboratory was used by means of the Levenberg–Marquardt and Universal Global Optimization (UGO) methods to generate all the regression parameters. Then validation was carried out to evaluate the resulting model with R^2 and root mean square error (RMSE) statistics at the L band (1.25 GHz) and 15 GHz, respectively. Next, the use of the improved dielectric model at moderate frequency is discussed. We propose that, combined with more experiments, measured data and scattering model, the improved dielectric model can be used for monitoring soil salinity on a regional basis with SAR remote sensing technology.

Laboratory experimentation

Soil samples preparation and measurements

Although the chemical compositions of soil can be very complex, sodium is ubiquitous. To determine the dielectric properties of moist saline soil, and to validate the improved model, five types of soil matrices (with different mechanical and structural compositions) were chosen and prepared as with varying moisture and salinity contents. There were 30 different samples for each of the five soil types resulting in 150 soil samples. The samples were stored in deep round aluminium cups with fixed uniform volume, compressed, and dried in an oven at 105°C. Deionized water was gradually added to the dried soil samples to divide them into 5 groups with moisture contents of 10, 15, 20, 25, and 30 ($cm^3\ cm^{-3}$). Each group included 6 soil samples with a NaCl solution at a concentration of 0, 2, 4, 8, 20, and 40 ($g\ kg^{-1}$). It must be pointed out that it is not easy to specify the prepared soil samples as saturated soil and saline soil because this is strictly dependent on soil structural property. But generally, the samples with moisture of 30 $cm^3\ cm^{-3}$ were approaching the saturated level, and samples with salinity of 2, 4, and 8 ($g\ kg^{-1}$) were called mild, moderate, and severe salinization, respectively. It was essential to keep prepared soil samples in the aluminium cups for 48 hours to make the samples homogeneous and allow the complete mixture of the soil and saline solutions. The aluminium cups held the soil samples and kept them away from air and any other external

interference. **Table 1** provides the mechanical and structural compositions of the five types of soil matrices.

Measurements of the complex dielectric constant of the samples were conducted using an HP85070B dielectric probe (Shao et al., 2003). The HP Dielectric Probe Kit (Model 85070B) consists of an open-ended semirigid coaxial cable connected to the dielectric probe and to a HP 8510C Network Analyzer by means of the HP 8517B *S*-parameter test set. The Dielectric Probe Kit software assists in data acquisition and permittivity calculations. A measurement system based on the 85070B dielectric probe outputs dielectric constant, loss factor, and loss tangent versus frequency — from 200 MHz to 20 GHz. The probe system was calibrated with a standard calibration procedure (air-short-deionized water) and refreshed daily up to three times during the measurement period. Hewlett-Packard states that the typical dielectric measurement accuracy is about ε' ±5%, loss tangent, tand $= \varepsilon''/\varepsilon'$; ±0.05%. Each measurement was repeated three times to reduce experimental errors.

Table 1. The mechanical and structural compositions of the five types of soil matrices used to prepare to soil samples with different moisture and salinity levels.

Region	Sand volume (%)	Silt volume (%)	Clay volume (%)	Texture
I (soil 1)	44.84	53.85	1.31	Silt loam
II (soil 2)	20.84	78.14	1.02	Silt loam
III (soil 3)	4.79	75.82	19.39	Silt soil
IV (soil 4)	11.98	52.0	36.02	Silty clay
V (soil 5)	4.83	54.5	40.67	Clay loam

Note: Soils 1–5 were collected from Qichuan, Luoyang city; Ling county, Shandong province; West mountain, Luoyang city; Wenfu city, Hunan province; and Shilingke village, Luoyang city, respectively.

Measured dielectric property of moist saline soil samples

Figure 1 shows the relationships between ε' and both moisture and salinity as a function of frequency (in logarithmic scale). Generally, ε' gradually decreases with an increase in frequency range from 200 MHz to 20 GHz and ε' also rapidly increased as moisture (m_v) increased. Note that salinity had a less marked effect. It is proposed that moisture is therefore a bigger influence on ε' when compared with salinity. In the moisture range from 10 to 30 (cm^3 cm^{-3}), ε' increases from 7.8 to 42, its highest value in each diagram, whereas the largest difference in ε' is only 20 as soil salinity varies from 0 to 40 (g kg^{-1}). Given the known

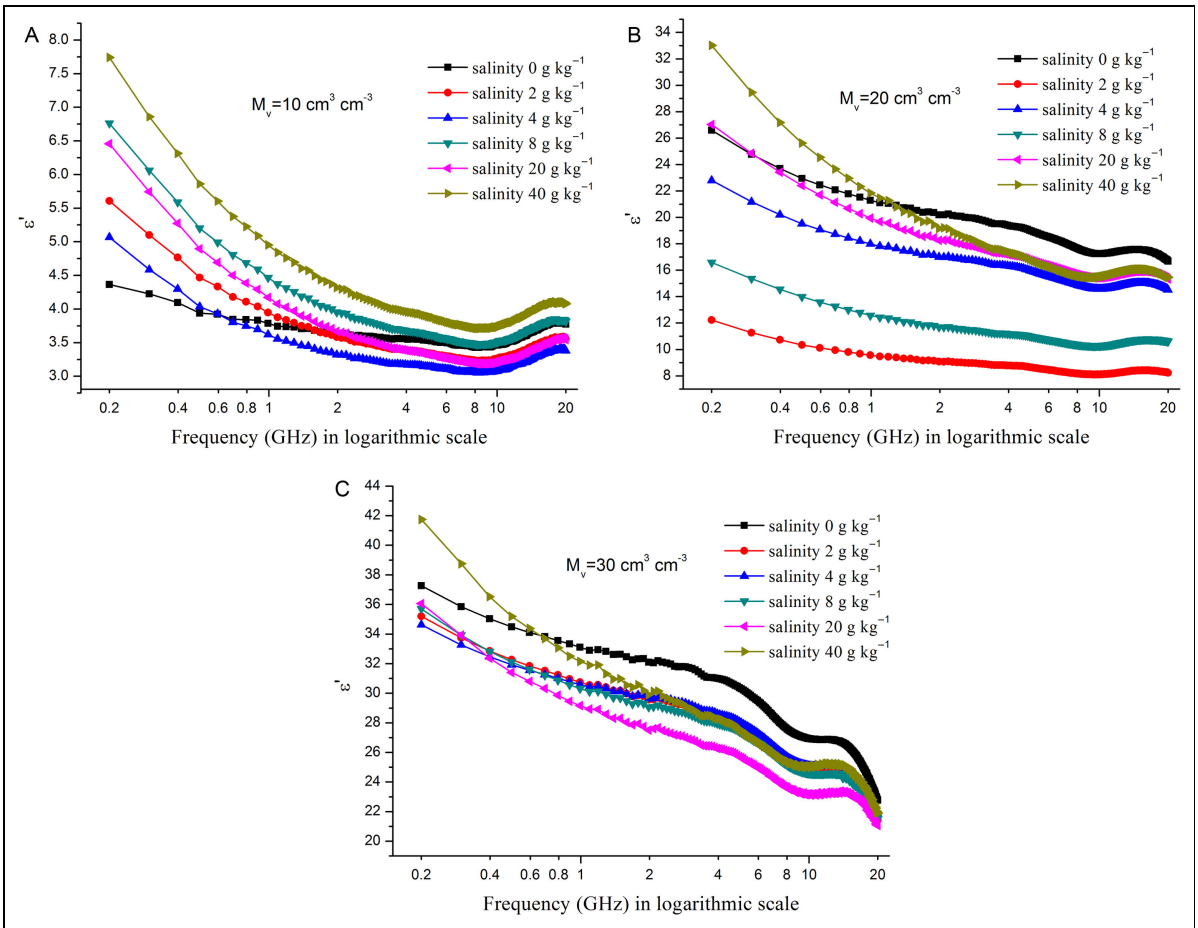

Figure 1. Relationships between ε' and both soil moisture (m_v) and salinity as a function of frequency (in logarithmic scale). Different colour curves denote the added saline solution concentrations (0, 2, 4, 8, 20, and 40 (g kg^{-1})).

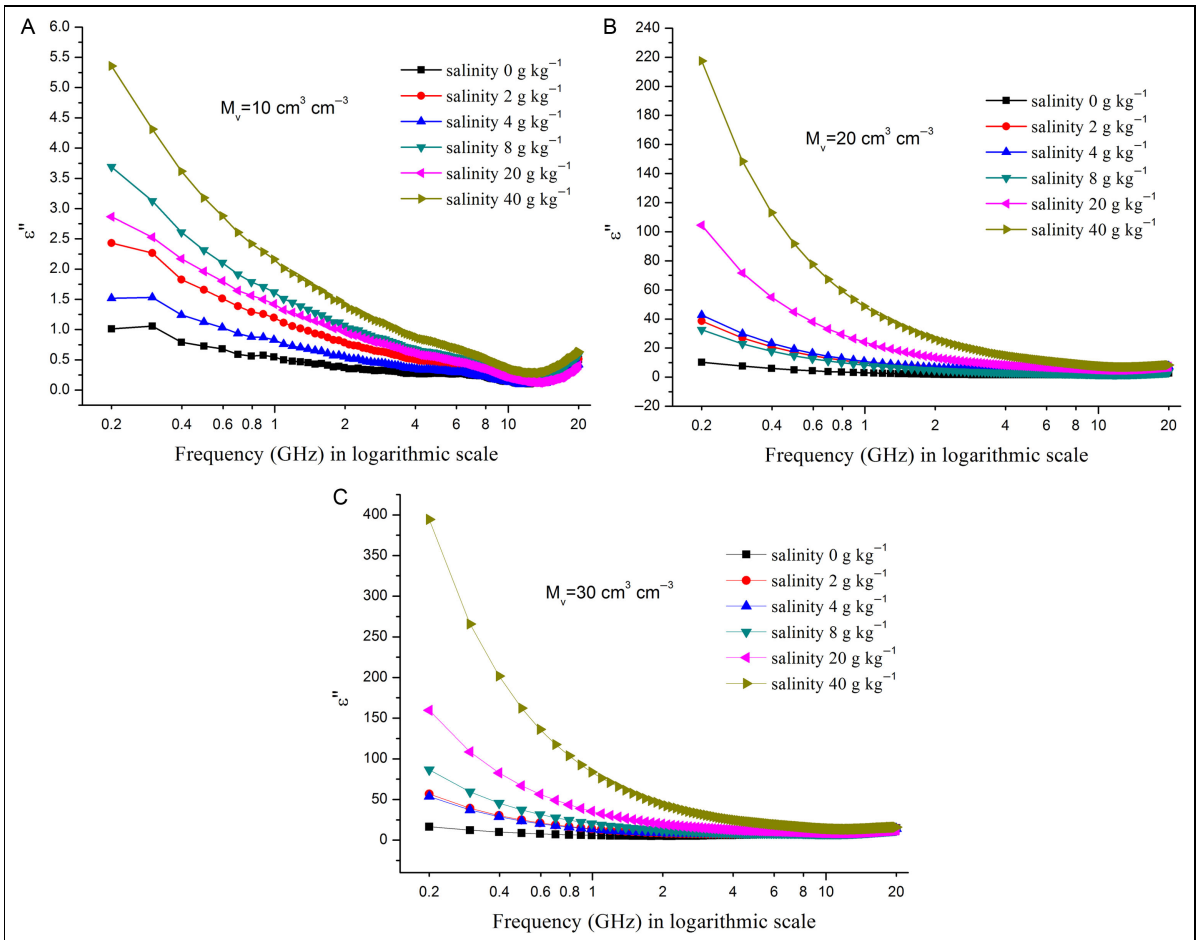

Figure 2. Relationships between ε'' and both soil moisture (m_v) and salinity as a function of frequency (in logarithmic scale). Different colour curves denote the added saline solution concentrations (0, 2, 4, 8, 20, and 40 (g kg^{-1})).

moisture levels, it is not clear how soil salinity affects ε'. This is because the salinity-influenced process on ε' is more complicated, and its contribution is usually small. This interpretation is in accord with the conclusions from Sreenivas et al. (1995), who pointed out that soil mechanical composition was another key factor influencing ε'.

Figure 2 shows the relationships between ε'' and both soil moisture and salinity as a function of frequency (in logarithmic scale). It shows that ε'' rapidly decreased with the increase of frequency in the lower frequency range (frequency $<$ 2 GHz). In the higher frequency range, soil salinity has little impact on ε'', and almost tends toward a constant value. Both soil salinity and moisture affect ε''. However, it is clear that salinity plays a more crucial role. For example, with a salinity of 40 g kg^{-1}, when soil moisture ranges from 10 to 30 (cm^3 cm^{-3}) the highest ε'' reaches 394 from 5.4. It is therefore proposed that moisture plays an auxiliary role to the contribution of salinity on ε''. Dried salt crystals have nearly the same dielectric property as dried soil minerals. However, when moisture increases salt crystals dissolve and generate salt ions, which increase conductivity. ε'' is usually viewed as attenuation, and higher conductivity can cause more loss of energy (including conductivity loss and relaxation loss), thus ε'' is higher. In addition, within the lower frequency range soil samples with different salinity have a more clearly defined different ε''. These results indicate a lower frequency can be more useful for salinity detection.

If the soil samples have low moisture, such as 5 and 10 (cm^3 cm^{-3}), the measurements are relatively noisy, as seen in the curves shown in **Figure 2** This is because at low moisture levels the distribution of water in the soil samples tends not to be homogeneous and uniform. And the electromagnetic waves could also penetrate drier soil and reach the aluminium cup, thus producing an unstable return signal.

Development of a salinity model

Dobson Semi-empirical Model

Dobson et al. (1985) developed a relatively simple, semi-empirical model as follows:

$$\varepsilon' = [1 + \frac{\rho_b}{\rho_s}(\varepsilon_s^{\alpha} - 1) + m_v^{\beta'}\varepsilon_{\mathrm{fw}}'^{\alpha} - m_v]^{1/\alpha} \quad (1)$$

$$\varepsilon'' = [m_v^{\beta''} \varepsilon_{\mathrm{fw}}''^{\alpha}]^{1/\alpha} \quad (2)$$

where m_v is moisture of the mixture in percent, ρ_b is the bulk density in grams per cubic centimetre, $\rho_s = 2.66\ \mathrm{g\ cm^{-3}}$ is the specific density of the soil solids, $\varepsilon_s = 4.7$ is the relative permittivity of the soil solids, $\alpha = 0.65$ is an empirically determined constant (shape factor), and β' and β'' are empirically determined soil-type dependent constants. The quantities $\varepsilon'_{\mathrm{fw}}$ and $\varepsilon''_{\mathrm{fw}}$ are the real and imaginary parts of the dielectric constant of free water, given by a Debye-type dispersion formula, with the latter modified to include a term that accounts for the effective conductivity of the soil mixture

$$\varepsilon'_{\mathrm{fw}} = \varepsilon_{w\infty} + \frac{\varepsilon_{w0} - \varepsilon_{w\infty}}{1 + (2\pi f \tau_{\mathrm{w}})^2} \quad (3)$$

$$\varepsilon''_{\mathrm{fw}} = \frac{2\pi f \tau_w (\varepsilon_{w0} - \varepsilon_{w\infty})}{1 + (2\pi f \tau_w)^2} + \frac{\sigma_{\mathrm{eff}}}{2\pi\varepsilon_0 f} \frac{(\rho_s - \rho_b)}{\rho_s m_v} \quad (4)$$

where $\varepsilon_{\mathrm{w0}} = 80.1$ (temperature (T) = 20 °C) is the static dielectric constant for water, $\varepsilon_{w\infty} = 4.9$ is the high-frequency limit of $\varepsilon'_{\mathrm{fw}}$, τ_w is the relaxation time for water, σ_{eff} is the effective conductivity in terms of the textural properties of the soil, and $\varepsilon_0 = 8.85 \times 10^{-12}\ \mathrm{F\ m^{-1}}$ is the permeability of free space.

Using soil samples prepared in the laboratory, the Dobson model should coincide well with the measured data. However, the model for treating the uncertainties of the dielectric constant of bound water used an approximation as follows:

$$m_v^{\beta'} \varepsilon_{\mathrm{fw}}'^{\alpha} = V_{\mathrm{fw}} \varepsilon_{\mathrm{fw}}'^{\alpha} + V_{\mathrm{bw}} \varepsilon_{\mathrm{bw}}'^{\alpha} \quad (5)$$

Because $m_v = V_{\mathrm{fw}} + V_{\mathrm{bw}}$, it follows that,

$$\begin{aligned} m_v^{\beta'} \varepsilon_{\mathrm{fw}}'^{\alpha} &= (m_v - V_{\mathrm{bw}})\, \varepsilon_{\mathrm{fw}}'^{\alpha} + V_{\mathrm{bw}} \varepsilon_{\mathrm{bw}}'^{\alpha} = m_v \varepsilon_{\mathrm{fw}}'^{\alpha} + V_{\mathrm{bw}} (\varepsilon_{\mathrm{bw}}'^{\alpha} - \varepsilon_{\mathrm{fw}}'^{\alpha}) \\ &\because \varepsilon'_{\mathrm{bw}} < \varepsilon'_{\mathrm{fw}} \therefore m_v^{\beta'} \varepsilon_{\mathrm{fw}}'^{\alpha} < m_v \varepsilon_{\mathrm{fw}}'^{\alpha} \\ &\Rightarrow \because 0 < m_v < 1 \therefore \beta' > 1 \end{aligned} \quad (6)$$

However, based on the measured data from Dobson et al. (1985), sometimes the opposite $\beta' < 1$ was obtained. This shows that empirical formulas are not suitable all the time, especially for coarse textured soil. In this study, β' was regarded as a regression parameter with a physical range. The same problem and solution also was found for β''. In addition, the shape factor (α) was used to describe dielectric behavior of solid soil (ε_s) and free water ($\varepsilon_{\mathrm{fw}}$). However, α should not be the same throughout the model, as the solid-liquid two phases had different influence factors, and α was not suitable for use as an influence as a fixed value in real and imaginary parts of the dielectric constant (Equations (1) and (2)).

Furthermore, the Dobson model was based on nonsaline soil samples as it does not include a salinity factor. Salinity in soil representing energy loss is usually dissolved in free water, because these salt ions can move about freely. Thus, in this study, the free water term in the Dobson model was replaced with the saline water term using the Stogryn model (Stogryn, 1970). Taking soil physics into account, an improved dielectric model for moist saline soil could be developed.

Stogryn model for saline water

Stogryn (1970) developed equations for calculating the dielectric constant of saline water (sw). The dielectric constant of saline water can be calculated in terms of temperature and salinity. These detailed equations are as follows,

$$\varepsilon'_{\mathrm{sw}} = \varepsilon_{\mathrm{sw}\infty} + \frac{\varepsilon_{\mathrm{sw0}} - \varepsilon_{\mathrm{sw}\infty}}{1 + (2\pi f \tau_{\mathrm{sw}})^2} \quad (7)$$

$$\varepsilon''_{\mathrm{sw}} = \frac{2\pi f \tau_{\mathrm{sw}} (\varepsilon_{\mathrm{sw0}} - \varepsilon_{\mathrm{sw}\infty})}{1 + (2\pi f \tau_{\mathrm{sw}})^2} + \frac{\sigma_i}{2\pi\varepsilon_0 f} \quad (8)$$

$$\varepsilon_{\mathrm{sw0}}(T, N) = \varepsilon_{\mathrm{sw0}}(T, 0)\, a(N) \quad (9)$$

$$2\pi\tau_{\mathrm{sw}}(T, N) = 2\pi\tau_{\mathrm{sw}}(T, 0) b(N, T) \quad (10)$$

$$\sigma_i(T, N) = \sigma_i(25, N) c(\Delta, T) \quad (11)$$

where $\varepsilon_{\mathrm{sw0}}(\mathrm{T}, 0) = \varepsilon_{w0}(\mathrm{T}, 0)$, $\varepsilon_{\mathrm{sw}\infty} = \varepsilon_{w\infty} = 4.9$, $\tau_{\mathrm{sw}}(\mathrm{T}, 0) = \tau_w(\mathrm{T}, 0)$, σ_i is conductivity of saline water, T is temperature in °C and $\Delta = 25 - \mathrm{T}$, and N is normality, which can be obtained in terms of salinity (Stogryn, 1970).

The terms $a(N)$, $b(N, \mathrm{T})$, $c(\Delta, \mathrm{T})$ are high-order polynomials from Stogryn (1970). To simplify calculating procedures, some approximations about polynomials were used in this study. Soil salinity is usually within a certain range and thus parameter N derived from the salinity is between 0 and 5. In this small range of N, the simulated curve based on the polynomials from Stogryn (1970) could almost be approximated as a straight line. Thus, the auxiliary parameters a and b could be fitted linearly with both correlation coefficients larger than 0.97.

$$a(N) = 0.962 - 0.157N \quad (12)$$

$$b(N) = 1.013 - 0.0625N \quad (13)$$

For σ_i, Stogryn (1970) proposed a high-order polynomial of salinity, and for the same reason, the small range of N in soil σ_i can be calculated using $\sigma_i = \zeta N$ form, where ζ is the first order fitting coefficient. As for the soil system, σ_i should be converted to conductivity of soil, and in this study a phenomenological equation was used, which means soil conductivity was produced by the free salt ions dissolved in the free water of soil.

$$\sigma = \zeta \frac{\rho_b S^{\psi}}{m_v^{\upsilon}} \quad (14)$$

where S and m_{v} are salinity and moisture of soil in percent, and ζ, ψ, and υ are the first order fitting coefficients. Note that salinity and moisture in soil are shown as two phases, free and bound, and only salt matter dissolved in free water was used for calculating σ. To describe partial salt matter dissolved in parts of soil water, further producing conductivity, ψ and υ are restricted to larger than 1.

Dielectric behavior model of moist saline soil

The real part of the model is primarily the same as the corresponding equation in the Dobson model. But, considering the α problem stated previously, another shape factor α' and α'', which are different from α, were used as independent parameters for the liquid phase in the real part and imaginary part equations. Note β' is within its range of larger than 1 as not all the water in soil exists as free phase. Thus, based on Equations (1) and (7), the real part of dielectric constant for moist saline soil is listed as

$$\varepsilon' = [1 + \frac{\rho_b}{\rho_s}(\varepsilon_s^{\alpha} - 1) + m_v^{\beta'}\varepsilon_{\mathrm{sw}}^{\prime\alpha'} - m_v]^{1/\alpha} \tag{15}$$

where α' and $\beta' > 1$ are regression parameters. Note that $\varepsilon_{\mathrm{sw}}^{\prime\alpha'}$ is different from the corresponding term in the Dobson model.

For ε'', research has shown that at low frequency conductivity loss plays a bigger role. When the frequency gets higher, relaxation loss is more important. Combining with this point and the method of Taylor series expansion, the model of ε'' is generated as a relatively simple form.

Using Equations (8), (12), (13) and (14), it follows that

$$\begin{aligned}\varepsilon''_{\mathrm{sw}} &= \frac{2\pi f \tau_{\mathrm{sw}}(T,0)\ b(N,T)[\varepsilon_{\mathrm{sw0}}(T,0)\ a(N) - \varepsilon_{\mathrm{sw}\infty}]}{1 + [2\pi f \tau_{\mathrm{sw}}(T,0)\ b(N,T)]^2} \\ &\quad + \frac{\sigma}{2\pi\varepsilon_0 f} = A + B\end{aligned} \tag{16}$$

where the A represents relaxation loss and B is conductivity loss. Then based on Equation (2), $\varepsilon_{\mathrm{fw}}^{\prime\prime\alpha}$ is replaced with $\varepsilon_{\mathrm{sw}}^{\prime\prime\alpha''}$, and the imaginary part of dielectric constant for moist saline soil is listed as

$$\varepsilon'' = m_v^{\beta''/\alpha}(A + B)^{\alpha''/\alpha} \tag{17}$$

where ζ, $\psi > 1$, and $\upsilon > 1$ are contained in B, and α'', $\beta'' > 1$ are regression parameters.

At low frequency $A << B$ and the Taylor series expansion of relaxation loss term is taken.

$$\begin{aligned}\varepsilon''_{\mathrm{low}} &= m_v^{\beta''/\alpha}[B^{\alpha''/\alpha} + B^{\alpha''/\alpha}\frac{\alpha''}{\alpha B}A + \mathrm{O}(A^2)] \\ &= m_v^{\beta''/\alpha}B^{\alpha''/\alpha} + m_v^{\beta''/\alpha}B^{\alpha''/\alpha}\frac{\alpha''}{\alpha B}A\end{aligned} \tag{18}$$

At high frequency, $A >> B$ and the Taylor series expansion of conductivity loss term is taken.

$$\begin{aligned}\varepsilon''_{\mathrm{high}} &= m_v^{\beta''/\alpha}[A^{\alpha''/\alpha} + A^{\alpha''/\alpha}\frac{\alpha''}{\alpha A}B + \mathrm{O}(B^2)] \\ &= m_v^{\beta''/\alpha}A^{\alpha''/\alpha} + m_v^{\beta''/\alpha}A^{\alpha''/\alpha}\frac{\alpha''}{\alpha A}B\end{aligned} \tag{19}$$

Thus, an improved model for dielectric behavior of moist saline soil at microwave frequencies was developed (with two groups of equations at low and high frequency).

Note that there is no precise definition for the boundary between low and high frequencies, as the application of Equations (18) or (19) depends on the comparison between conductivity loss and relaxation loss contributions, which are more related to the actual composition and structure of the soil matrix. Further analysis of this relationship based on specific cases is required. The following section contains a detailed discussion on how to use the improved dielectric model at a moderate frequency.

Model validation and analysis

To generate all the regression parameters of the improved model, a part of the data measured from the soil samples in the laboratory was used by means of the Levenberg–Marquardt and UGO methods. Levenberg–Marquardt is a virtual standard in nonlinear optimization that significantly

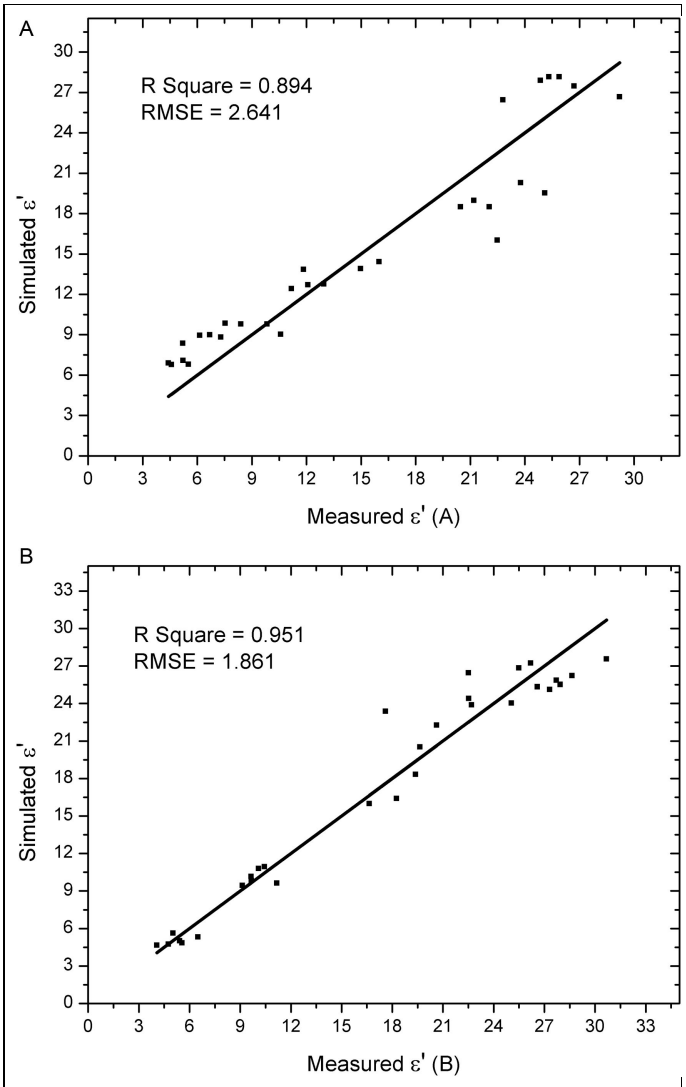

Figure 3. Relationships between the measured and simulated real part of the dielectric constant (ε') for soil 1 (A) and soil 4 (B) at the C band (5.25 GHz) based on Equation (15). The solid line in each diagram accounts for the 1:1 line, and R^2 and RMSE are shown.

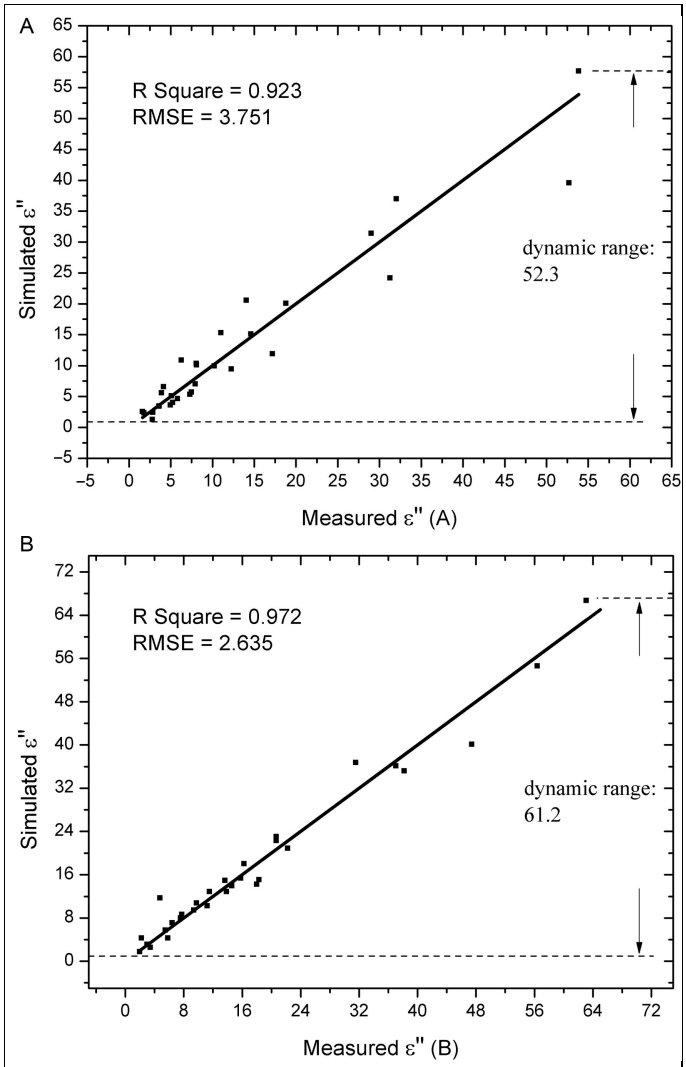

Figure 4. Relationships between the measured and simulated imaginary part of the dielectric constant (ε'') for soil 1 (A) and soil 4 (B) at the L band (1.25 GHz) based on Equation (18). The solid line in each diagram accounts for the 1:1 line, and R^2 and RMSE are shown. The dashed line represents the dynamic range of ε''.

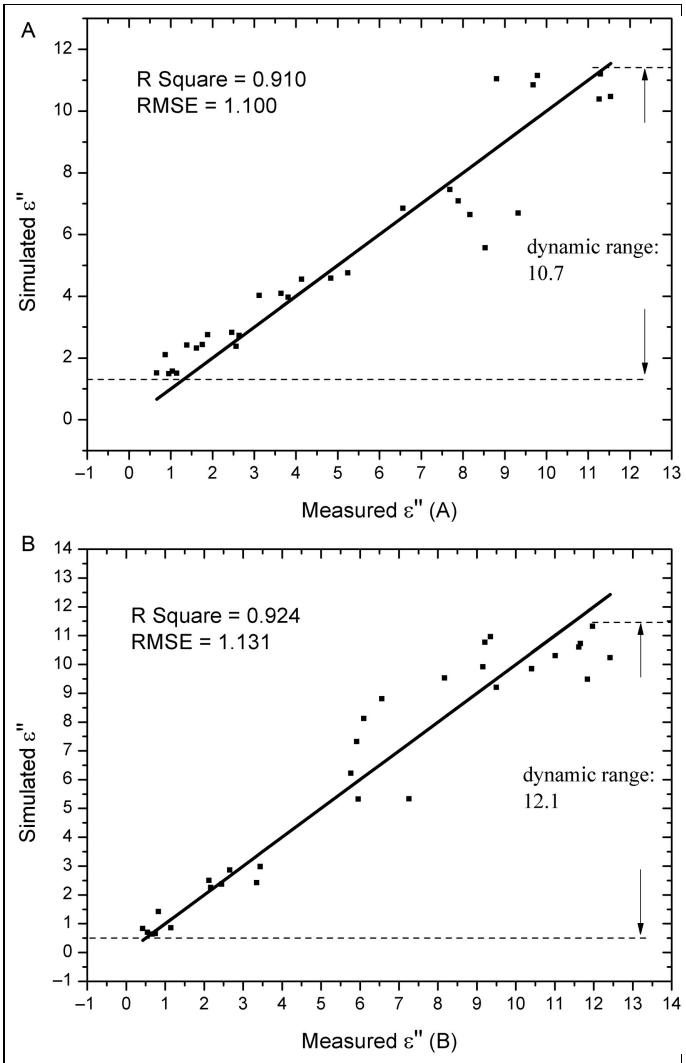

Figure 5. Relationships between the measured and simulated imaginary part of the dielectric constant (ε'') for soil 1 (A) and soil 4 (B) at 15 GHz based on Equation (19). The solid line in each diagram accounts for the 1:1 line, and $R^2$and RMSE are shown. The dashed line represents the dynamic range of ε''.

outperforms gradient descent and conjugate gradient methods for medium sized problems. The most important feature of UGO is to overcome the problem that an iterative method must be given an appropriate initial value. UGO can converge rapidly to the optimal value based on a random initial value. The combination of the two algorithms can facilitate the model building.

After the model was built, the dielectric constant of moist saline soil could be simulated, with moisture (m_v), salinity (S), bulk density (ρ_b), temperature (T), and frequency (f) as input parameters. The remainder of the measured data from the soil samples was used to carry out model validation and analysis. Only soil 1 and soil 4 were used for this analysis because the two types of soil matrices have markedly different mechanical and structural compositions (**Table 1**).

Figure 3 shows the comparison between measured ε' and simulated ε' at C band (5.25 GHz). Note the fit is good. The R^2 and RMSE are, respectively, 0.894 and 2.641 (soil 1) and 0.951 and 1.861(soil 4). For other frequencies such as L band (1.25 GHz) good results can be also obtained. That indicates that Equation (15) can portray ε' of moist saline soil, independent of frequency. In addition, it also explains that salinity makes a small contribution to ε', as in Equation (15) only ε'_{sw} considers the salinity factor and usually the effect of salinity on ε'_{sw} can be ignored. This shows that detection of soil salinity is impossible using only ε'.

From the plots in **Figure 4**, it follows that the simulated ε'' aligns well with the measured data in Equation (18) at L band (1.25 GHz). It must be pointed out that Equation (18) has a salinity multiplying factor because of the Taylor series expansion of the relaxation loss term. When salinity is close

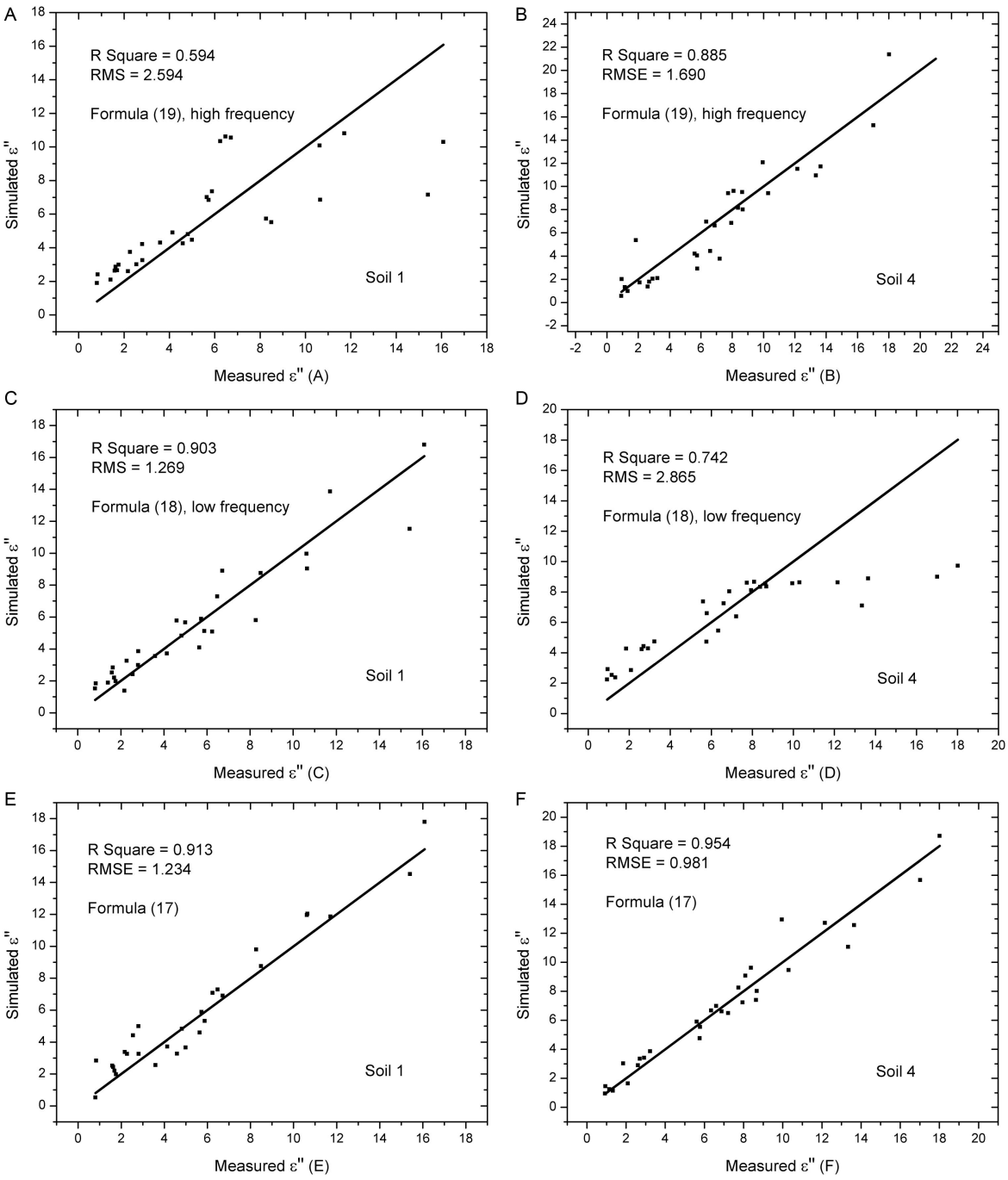

Figure 6. Relationships between the measured and simulated imaginary part of the dielectric constant (ε'') for soil 1 (A, C, E) and soil 4 (B, D, F) at C band (5.25 GHz) based on Equations (18), (19), and (17), respectively. The solid line in each diagram accounts for the 1:1 line, and $R^2$and RMSE are shown.

to zero, calculated ε'' approximates zero. Thus, Equation (18) is not suitable to nonsaline soil, and it should be modified using an unsimplified Equation (17). Research has shown that L band, or a lower frequency, is the optimal configuration for detecting soil salinity. Compared with ε'' in **Figures 4** and **5**, it has been found that the dynamic range of ε'' at L band is largest. This indicates that L band can detect ε'' changing more easily and accurately.

Equation (19) was used at 15 GHz, and **Figure 5** shows a good fitting effect both for soil 1 and soil 4, which supports the modeling idea of Equation (19).

Moreover, dielectric property is also controlled by the structure of soil matrix, and because of the difference of soil matrix, the importance between conductivity loss and relaxation loss cannot be determined easily at a moderate frequency such as C band around 5.25 GHz. The Taylor

series expansion cannot be used to simplify the equations without reason.

Figure 6 shows the relationships between measured and simulated ε'' for soil 1 (A, C, E) and soil 4 (B, D, F) at C band (5.25 GHz) based on Equations (18), (19), and (17), respectively. Based on the comparison between **Figures 6A** and **6B**, soil 4 represented a relatively better result. This is because soil 4 had higher clay content than soil 1 (**Table 1**), and the free water content for soil 4 was accordingly smaller due to its stronger soil adsorption. The influence of salinity on ε'' lies on the salt matter dissolved in free water, and this is the reason why **Figures 6 A** and **6B** show such contrasting results.

Equation (18) for low frequency was also used at C band (**Figures 6C** and **6D**), and it appeared that simulated accuracy for soil 1 was improved; however, the accuracy for soil 4 was reducing. The reason is that Equation (18) emphasizes conductivity loss, which strongly depends on the free water content in the soil matrix. For moderate frequency or complicated structure of the soil matrix Equation (17) should be used, which takes into account the two-sided influence factors simultaneously (**Figures 6E** and **6F**).

Through the analysis presented, the improved dielectric model of moist saline soil can simulate the soil dielectric behavior well at low and high frequencies. Because low frequency is conducive to salinity detection, development of procedures for soil salinity detection is possible. It should also be pointed out that to further develop a more compact and applicable model, all the regression parameters should be calculated based on properties of the soil matrix and not using optimization methods. However, the five types of soil matrices used in this paper are not enough to provide empirical formula for regression parameters, and more research and analysis are necessary.

Conclusions

Using soil samples prepared in the laboratory, the notable factors influencing the real and imaginary parts of the dielectric constant were summarized. Then, a physically based model was developed and validated. Key findings were the technique proposed for replacing the free water term in the Dobson model with the saline water term used in the Stogryn model, and some approximations were also used in simplifying the calculations. Then, according to the laws of dielectric behavior of soil, the Taylor series expansion was applied for further simplifications. Thus, an improved model for dielectric behavior of moist saline soil was developed.

With data from the 150 soil samples prepared in the laboratory, building and validation of the improved dielectric model was done based on the Levenberg–Marquardt and UGO methods. The results showed that the fitting effect, as a whole, is good. For example, discussion on how to use the improved dielectric model at moderate frequency (C band (5.25 GHz)) was conducted.

The study also proposed that lower frequency, such as L band (1.25 GHz), can be more useful for salinity detection based on measured data of prepared soil samples. ε'' rapidly decreased in the lower frequency range (**Figure 2**). However at the C band (5.25 GHz), under the condition of the fixed moisture, different salinity samples could not produce clearly different ε''.

It is anticipated that SAR can become a useful tool to detect salinity based on the combination of the scattering model and the dielectric model. Before that can happen, there is a need to obtain more measured data to develop a more compact and applicable model. All the regression parameters should be calculated based on properties of the soil matrix and not using optimization methods. Rigorous experiments under varying field conditions and further development of inversion algorithm is the next area of research interest.

Acknowledgement

The authors would like to take this opportunity to express their sincere appreciation to the anonymous reviewers. This study is supported by CAS Knowledge Innovation Program (KZCX2-EW-320), the National High Technology Research and Development Program (2007AA12Z168), National Natural Science Foundation (41201346), and IRSA/CAS (Y1S01200CX).

References

Aly, Z., Bonn, F.J., and Magagi, R. 2007. Analysis of the backscattering coefficient of salt-affected soils using modeling and RADARSAT-1 SAR data. *IEEE Transactions on Geoscience Remote Sensing*, Vol. 45, No. 2, pp. 332–341. doi: 10.1109/TGRS.2006.887163.

Dobson, M.C., Ulaby, F.T., Hallikainen, M.T., and El-Rayes, M.A. 1985. Microwave dielectric behavior of wet soil — Part 2: Dielectric mixing models. *IEEE Transactions on Geoscience Remote Sensing*, Vol. 23, No. 1, pp. 35–46. doi: 10.1109/TGRS.1985.289498.

Dubois, P.C., Van, Z.J., and Engman, E.T. 1995. Measuring soil moisture with imaging radars. *IEEE Transactions on Geoscience Remote Sensing*, Vol. 33, No. 4, pp. 915–926. doi: 10.1109/36.406677.

Fariften, J., Farshad, A., and George, R.J. 2006. Assessing salt-affected soils using remote sensing, solute modelling, and geophysics. *Geoderma*, Vol. 130, No. 3, pp. 19–206.

Fung, A.K., Li, Z., and Chen, K.S. 1992. Backscattering from a randomly rough dielectric surface. *IEEE Transactions on Geoscience Remote Sensing*, Vol. 30, No. 2. pp. 356–369. doi: 10.1109/36.134085.

Hallikainen, M.T., Ulaby, F.T., Dobson, M.C., El-Rayes, M.A., and Wu, L.K. 1985. Microwave dielectric behavior of wet soil — Part 1: empirical models and experimental observations. *IEEE Transactions on Geoscience Remote Sensing*, Vol. 23, No. 1, pp. 25–34. doi: 10.1109/TGRS.1985.289497.

Lasne, Y., Paillou, P., Freeman, A., Farr, T., Mcdonald, K.C., Ruffié, G., Malézieux, J., Chaoman, B., and Demontoux, F. 2008. Effect of salinity

on the dielectric properties of geological materials: implication for soil moisture detection by means of radar remote sensing. *IEEE Transactions on Geoscience Remote Sensing*, Vol. 46, No. 6. pp. 1674–1688. doi: 10.1109/TGRS.2008.916220.

Lesch, S.M., Rhoades, J.D., Lund, L.J., and Corwin, D.L. 1992. Mapping soil salinity using calibrated electromagnetic measurements. *Soil Science Society of America Journal*, Vol. 56, No. 2, pp. 540–548. doi: 10.2136/sssaj1992.03615995005600020031x.

Metternicht, G.I. 1998. Fuzzy classification of JERS-1 SAR data: an evaluation of its performance for soil salinty mapping. *Ecological Modelling*, Vol. 111, No. 1, pp. 61–74. doi: 10.1016/S0304-3800(98)00095-7.

Metternicht, G.I., and Zinck, J.A. 2003. Remote sensing of soil salinity: potentials and constraints. *Remote Sensing of Environment*, Vol. 85, No. 1, pp. 1–20. doi: 10.1016/S0034-4257(02)00188-8.

Mironov, V.L., Dobson, M.C., Kaupp, V.H., Komarov, S.A., and Kleshchenko, V.N. 2004. Generalized refractive mixing dielectric model for moist soils. *IEEE Transactions on Geoscience Remote Sensing*, Vol. 42, No. 4. pp. 773–785. doi: 10.1109/TGRS.2003.823288.

Oh, Y., Sarabandi, K., and Ulaby, F.T. 1992. An empirical model and an inversion technique for radar scattering from bare soil surfaces. *IEEE Transactions on Geoscience Remote Sensing*, Vol. 30, No. 2, pp. 370–381. doi: 10.1109/36.134086.

Peplinski, N.R., Ulaby, F.T., and Dobson, M.C. 1995. Dielectric properties of soils in the 0.3-1.3-GHz range. *IEEE Transactions on Geoscience Remote Sensing*, Vol. 33, No. 3, pp. 803–807. doi: 10.1109/36.387598.

Schmullius, C., and Evans, L. 1997. Tabular summary of SIR-C/X-SAR results: SAR frequency and polarization requirements for applications in ecology and hydrology. *IEEE Geoscience and Remote Sensing Symposium*, Vol. 4, pp. 1734–1736.

Shao, Y., Hu, Q., Guo, H., Lu, Y., Dong, Q., and Han, C. 2003. Effect of dielectric properties of moist salinized soils on backscattering coefficients extracted from RADARSAT image. *IEEE Transactions on Geoscience Remote Sensing*, Vol. 41, No. 8, pp. 1879–1888. doi: 10.1109/TGRS.2003.813499.

Shi, J., Wang, J., Hsu, A.Y., O'neill, P.E., and Engman, T. 1997. Estimation of bare surface soil moisture and surface roughness parameter using L-band SAR image data. *IEEE Transactions on Geoscience Remote Sensing*, Vol. 35, No. 5, pp. 1254–1265. doi: 10.1109/36.628792.

Sreenivas, K., Venkataratnam, L., and Narasimha Rao, P.V. 1995. Dielectric properties of salt-affected soils. *International Journal of Remote Sensing*, Vol. 16, No. 4, pp. 641–649. doi: 10.1080/01431169508954431.

Stogryn, A. 1970. Equations for calculating the dielectric constant of saline water. IEEE Trans. Microw. Theory. Vol. MIT-19, pp. 733–736.

Taylor, G.R., Mah, A.H., Kruse, F.A., Kierein-Young, K.S., Hewson, R.D., and Bennett, B.A. 1996. Characterization of saline soils using airborne radar imagery. *Remote Sensing of Environment*, Vol. 57, No. 3, pp. 127–142. doi: 10.1016/0034-4257(95)00239-1.

Triantafilis, J., Odeh, I.O.A., and McBratney, A.B. 2001. Five geostatistical models to predict soil salinity from electromagnetic induction data across irrigated cotton. *Soil Science Society of America Journal*, Vol. 65, No. 3, pp. 869–878. doi: 10.2136/sssaj2001.653869x.

Triantafilis, J., and Lesch, S.M. 2005. Mapping clay content variation using electromagnetic induction techniques. *Computers and Electronics in Agriculture*, Vol. 46, No. 1, pp. 203–237. doi: 10.1016/j.compag.2004.11.006.

Tsang, L., Kong, J.A., and Shin, R.T. 1985. *Theory of Microwave Remote Sensing*. John Wiley & Sons, New York.

Ulaby, F.T., Moore, R.K., and Fung, A.K. 1981. *Microwave Remote Sensing: Active and Passive*. Artech House, Norwood, MA.

Van Dam, R.L., Borchers, B., and Hendrickx, J.M.H. 2005. Methods for prediction of soil dielectric properties: a review, Detection and Remediation Technologies for Mines and Minelike Targets X. Proc. SPIE Vol. 5794, pp. 188–197. doi: 10.1117/12.602868.